



Semaphorin3d mediates Cx43-dependent phenotypes during fin regeneration

Quynh V. Ton, M. Kathryn Iovine*

Department of Biological Sciences, Lehigh University, 111 Research Drive, Iacocca B-217, Bethlehem, PA 18015, United States

ARTICLE INFO

Article history:

Received 21 October 2011

Received in revised form

14 March 2012

Accepted 20 March 2012

Available online 20 April 2012

Keywords:

Cx43

Semaphorin

Bone

Fin regeneration

Zebrafish

ABSTRACT

Gap junctions are proteinaceous channels that reside at the plasma membrane and permit the exchange of ions, metabolites, and second messengers between neighboring cells. Connexin proteins are the subunits of gap junction channels. Mutations in zebrafish *cx43* cause the *short fin* (*sof^{fb123}*) phenotype which is characterized by short fins due to defects in length of the bony fin rays. Previous findings from our lab demonstrate that Cx43 is required for both cell proliferation and joint formation during fin regeneration. Here we demonstrate that *semaphorin3d* (*sema3d*) functions downstream of Cx43. Semas are secreted signaling molecules that have been implicated in diverse cellular functions such as axon guidance, cell migration, cell proliferation, and gene expression. We suggest that *Sema3d* mediates the Cx43-dependent functions on cell proliferation and joint formation. Using both in situ hybridization and quantitative RT-PCR, we validated that *sema3d* expression depends on Cx43 activity. Next, we found that knockdown of *Sema3d* recapitulates all of the *sof^{fb123}* and *cx43*-knockdown phenotypes, providing functional evidence that *Sema3d* acts downstream of Cx43. To identify the potential *Sema3d* receptor(s), we evaluated gene expression of *neuropilins* and *plexins*. Of these, *npr2a*, *plxna1*, and *plxna3* are expressed in the regenerating fin. Morpholino-mediated knockdown of *plxna1* did not cause *cx43*-specific defects, suggesting that PlexinA1 does not function in this pathway. In contrast, morpholino-mediated knockdown of *npr2a* caused fin overgrowth and increased cell proliferation, but did not influence joint formation. Moreover, morpholino-mediated knockdown of *plxna3* caused short segments, influencing joint formation, but did not alter cell proliferation. Together, our findings reveal that *Sema3d* functions in a common molecular pathway with Cx43. Furthermore, functional evaluation of putative *Sema3d* receptors suggests that Cx43-dependent cell proliferation and joint formation utilize independent membrane-bound receptors to mediate downstream cellular phenotypes.

© 2012 Elsevier Inc. All rights reserved.

Introduction

Connexins are the subunits of gap junction channels that direct cell–cell communication of ions and metabolites (≤ 1200 Da). Each connexin is a four-pass transmembrane spanning domain protein. Six connexins oligomerize to form a hemichannel, or connexon. Two connexons dock at the plasma membrane of adjacent cells to form a complete gap junction channel. Gap junction intercellular communication (GJIC) contributes to numerous developmental processes, including skeletogenesis. For example, mutations in human *CX43* result in oculodentodigital dysplasia (ODDD, Paznekas et al., 2003). ODDD is an autosomal dominant disease causing craniofacial bone deformities and limb abnormalities (Paznekas et al., 2003; Flenniken et al., 2005). Skeletal defects in the *CX43^{-/-}* knockout mouse include

delayed ossification of the axial and craniofacial skeletons (Lecanda et al., 2000). However, the underlying mechanisms by which Cx43-based GJIC leads to skeletal disease phenotypes are largely unknown.

Importantly, the function of Cx43 in skeletal morphogenesis is conserved. Indeed, our lab has found that mutations in zebrafish *cx43* cause the *short fin* (*sof^{fb123}*) phenotype (Iovine et al., 2005). The *sof^{fb123}* mutant is characterized by defects in the length of the bony fin ray segments, leading to short fins. The *sof^{fb123}* allele exhibits reduced *cx43* mRNA levels without a lesion in the coding sequence (Iovine et al., 2005). However, three additional alleles generated by non-complementation express missense mutations that cause reduced GJIC (Hoptak-Solga et al., 2007). During fin regeneration, the *cx43* mRNA is up-regulated in the population of dividing cells. Indeed, all four *sof* alleles exhibit reduced levels of cell proliferation in addition to short segments (Hoptak-Solga et al., 2008). Furthermore, morpholino-mediated *cx43* knockdown completely recapitulates the reduced fin length, reduced segment length, and reduced cell proliferation phenotypes observed in the

* Corresponding author. Fax: +610 758 4004.

E-mail address: mki3@lehigh.edu (M. Kathryn Iovine).

sof alleles (Hoptak-Solga et al., 2008). Together, these data reveal that reduced mRNA expression (*sof*^{b123}), reduced protein expression (*sof*^{b123} and morpholino-mediated knockdown), or reduced Cx43-based GJIC (three missense alleles) cause the same set of phenotypes. Thus, we refer to any loss of Cx43 function as a loss of Cx43 activity.

Given the observation that any loss of Cx43 activity leads to both reduced cell proliferation and short segments, it may be natural to speculate that reduced cell proliferation causes short segments. However, reduced signaling via the Shh or Fgfr1 signaling pathways also causes reduced cell proliferation and reduced fin length, but does not influence segment length (Quint et al., 2002; Lee et al., 2005). Thus, reducing the level of cell proliferation is not sufficient to impact segment length. We suggest instead that Cx43 plays an additional role in the regulation of segment length, perhaps by regulating joint formation. Our analyses of the *another long fin* (*alf*^{dyt86}) mutant supports this hypothesis. In contrast to *sof*, the *alf*^{dyt86} mutant exhibits fin overgrowth and stochastic joint failure/overlong segments (van Eeden et al., 1996), phenotypes opposite to *sof*. Interestingly, our analyses revealed that *alf*^{dyt86} mutants over-express *cx43* mRNA (Sims et al., 2009). Furthermore, *cx43*-knockdown in *alf*^{dyt86} fins rescues overgrowth and segment length, suggesting that *cx43* over-expression is responsible for the *alf*^{dyt86} phenotypes (Sims et al., 2009). Based on these loss-of-function and gain-of-function phenotypes, we suggest that Cx43 activity both promotes cell proliferation and suppresses joint formation, thereby coordinating bone growth and skeletal patterning.

A long-standing question with regard to connexin mutations is, how do gap junctions influence tangible cellular outcomes such as cell proliferation and cell differentiation? One hypothesis is that Cx43-based GJIC influences gene expression (Stains et al., 2003). To identify global changes in gene expression occurring downstream of *cx43*, we utilized a novel microarray strategy. We focused on the subset of genes both down-regulated in *sof*^{b123} and up-regulated in *alf*^{dyt86} to enable the identification of *cx43*-dependent genes. Here we provide molecular and functional validation of one gene identified by this microarray, *semaphorin3d* (*sema3d*). Semas comprise a large family of evolutionarily conserved signaling molecules initially found to provide axonal guidance cues during patterning of the central nervous system (Kolodkin et al., 1992). More recent studies have revealed that semaphorins are expressed in most cell types and, in addition to patterning the nervous system, also contribute to vasculature, heart, lung, kidney, bone and tooth development (reviewed in Roth et al., 2009). Class 3 Semas, such as *Sema3d*, are secreted ligands that interact with several possible cell surface receptors in order to mediate downstream cellular outcomes including cell adhesion, cell migration, cell proliferation, cell viability, and gene expression (reviewed in Yazdani and Terman, 2006). Thus, the finding that a Semaphorin acts functionally downstream of Cx43 provides tangible

insights into how skeletal morphogenesis may be influenced by Cx43 activity.

Materials and methods

Fish maintenance

Zebrafish were raised at constant temperature of 25 °C with 14 light: 10 dark photoperiod (Westerfield, 1993). Wild-type (C32), *sof*^{b123} (Iovine and Johnson, 2000) and *alf*^{dyt86} (van Eeden et al., 1996) were used in this study.

RNA isolation, fluorescent cRNA synthesis and microarray hybridization

Total RNA of wild-type, *sof*^{b123} and *alf*^{dyt86} 5 dpa regenerating fins were extracted using Trizol (Invitrogen, San Diego). RNA quantity and quality were determined by nanodrop and Bioanalyzer 2100 (Agilent) analyses. Only samples in yield higher than 50 ng/μL RNA, having sharp 60S and 40S rRNA peaks shown in the Bioanalyzer electropherogram, and 260/280 ratios > 1.7 were used. Fluorescent cRNAs were generated using the Agilent Low RNA Input Linear Amplification Kit and Qiagen RNeasy mini columns to purify the fluorescent target. Experimental Cy5 labeled samples (*alf*^{dyt86}, *sof*^{b123}) were competitively hybridized against equal amounts of Cy3 labeled wild-type cRNAs on an Agilent 4 × 44 K zebrafish 60-mer oligo microarray (G25190F-015064). After washing the microarray was scanned in an Agilent microarray scanner and red (Cy5) and green (Cy3) signal intensities were evaluated and processed with Agilent Feature Extraction software (v 7.5). The relative expression value of a gene for two different samples was represented by base 2 log ratios of the two signal intensities. Further data normalization, transformation and filtering for differential gene expression were performed using Agilent Genespring GX (v7.5).

In situ hybridization

Probes were prepared from linear DNA generated from PCR products where the reverse primer contained the binding site for the T7 RNA polymerase (see Table 1 for sequences). Five days post amputation (dpa) regenerating fins from wild-type, *sof*^{b123}, or *alf*^{dyt86} were fixed overnight with 4% paraformaldehyde in PBS and dehydrated in 100% methanol at −20 °C. Gradual aqueous washes were completed in methanol/PBST. Fins were then treated with 5 μg/ml proteinase K for 45 min and re-fixed in 4% paraformaldehyde in PBS for 20 min. Extensive washes in PBST were followed by prehybridization process in HYB+ solution (HYB+ solution is 50% formamide, 5 X SSC, 10 mM citric acid, 0.1% Tween20, heparin and tRNA) at 65 °C for 30 min–1 h. Hybridization in the presence of

Table 1
Primer and morpholino sequences.

Gene	Primers for ISH	Morpholinos
<i>sema3d</i>	F-CGAAGTGTAGTACCATTTACG RT7-TAATACGACTCACTATAGGG-TATGAGGATCATATGTCC	MO-TGTCCGGCTCCCTGCAGTCTTCAT 5MM-TGTGCCGCTGCCCTCCACTCTTCAT
<i>nrp2a</i>	F-CCAGTCCAGTAACCAGCG RT7-TAATACGACTCACTATAGGGTCAAGCCTCGGAGCAGCAGC	MO-CCAGAAATCCATCTTTCCGAAATGT 5MM-CCACAAAACGATCTTTGCCAAATGT
<i>plxna1</i>	F-AAGTGTTCTCTCGGCGCAG RT7-TAATACGACTCACTATAGGG-TTGCCACCTCCGAAAAACC	MO-GCCACATATCTGCAGTGGTCTTTGA 5MM-GCCAGATATGTGGACTGCTCTCTCA
<i>plxna3</i>	F-AGTGTTCTCTAAAGCAAC RT7-TAATACGACTCACTATAGGG-CCGCTTTCTGGAGCCTC	MO-ATACCAGCAGCCACAAGGACCTCAT 5MM-ATACGACCAACCAGAAGCACTCAT

The RNA polymerase T7 binding site is underlined in the reverse primers.
MO=targeting morpholino; 5MM=control morpholino with 5 mismatch pairs to target sequence.

digoxigenin-labeled antisense probes was completed overnight at 65 °C. The next day, the fins were washed gradually in HYB to 2X SSC to 0.2X SSC and finally to PBST. Anti-digoxigenin Fab fragments (pre-absorbed against zebrafish tissue) were used at 1:5000 overnight. On day 3, extensive washes in PBST were performed before three short washes in staining buffer (100 mM Tris, 9.5, 50 mM MgCl₂, 100 mM NaCl, 0.1% Tween20, pH 9.0). Fins were next transferred to staining solution (staining buffer plus NBT and BCIP) and development proceeded until a purple color was observed. For final result, fins were then washed with PBST, pre-fixed in 4% paraformaldehyde in PBS and mounted onto microscope slides. Labeled fins were examined on a Nikon Eclipse 80i microscope. Images were collected using a digital Nikon camera.

Following whole mount in situ hybridization, fins were embedded in 1.5% agarose/5% sucrose, and equilibrated overnight in 30% sucrose. Fins were mounted in OCT and cryosectioned (18–20 µm sections) using a Reichert–Jung 2800 Frigocut cryostat. Sections were collected on Superfrost Plus slides (Fisher) and mounted in 100% glycerol.

Morpholino knockdown and electroporation

Injection and electroporation experiments were performed as described (Thummel et al., 2006; Hoptak-Solga et al., 2008; Sims et al., 2009). Targeting morpholinos were targeted against the start codon and modified with fluorescein (Gene Tools, LLC) to provide a charge and for detection. Sequences for the targeting and control morpholinos can be found in Table 1.

Adult fish were first anesthetized using Tricane-S. Fin amputation was performed under a dissecting microscope. At 3 dpa, morpholinos were injected using a Narishige IM 300 Microinjector. Approximately 50 nl of morpholino (i.e. targeting or control 5 mM morpholinos) was injected per ray (5–6 fin rays per fin, the other rays were uninjected control). Immediately following injection, both dorsal and ventral halves were electroporated using a CUY21 Square Wave Electroporator (Protech International, Inc.). The following parameters were used: ten 50-ms pulses of 15 V with a 1 s pause between pulses. At 24 hpe (hours post electroporation), success was evaluated by monitoring fluorescein uptake under fluorescence microscope. Fins were harvested either at 1 dpe for H3P detection and for qRT-PCR or at 4 dpe for ZNS5 detection. Three to five fins were injected per morpholino (i.e. targeting or mismatch); the un-injected side served as an independent control. Each morpholino was tested in at least three independent experiments to ensure reproducibility. The graphs in Fig. 2 are based combined data from two comparable experiments ($n=7$). Statistical significance was determined using the student's t -test ($p < 0.05$).

Immunofluorescence

Fins were harvested after morpholino knockdown experiments (for ZNS5 detection staining, fins were harvested 4 dpe; for H3P detection staining, fins were harvested 1 dpe). Fins were then fixed in 4% paraformaldehyde in PBS for 2 h at RT and then dehydrated in methanol. During processing, fins were washed gradually in methanol/PBS followed by 3 washes in block solution (50 ml PBS, 1 g BSA, 250 µl triton). Either the mouse ZNS5 (Zebrafish International Resource Center: <http://zebrafish.org/zirc/home/guide.php>, 1:200) or the rabbit antibody against histone-3-phosphate (anti-H3P, Millipore, 1:100) were incubated with fins overnight at 4 °C. Next day, antibodies were removed and fins were washed in block solution 3 × 10 min. Secondary antibodies (i.e. anti-mouse Alexa 488 for ZNS5 detection or anti-rabbit Alexa 546 for H3P detection) were diluted in 1:200 blocking solution and incubated overnight at 4 °C. Following 3 × 10 min treatment in blocking solution, fins were

washed in PBS and then mounted onto slides in glycerol. Labeled fins were examined on a Nikon Eclipse 80i microscope. Images were collected using a digital Nikon camera.

Measurements

Fins were imaged on a Nikon SMZ1500 dissecting microscope at 4X (regenerate length) or 10X (segment length or the number of dividing cells). Photographs were taken using a Nikon DXM1200 digital camera. For regenerate length, segment length, and the number of dividing cells, all measurements were taken from only the longest fin rays (i.e. the third ray from either the dorsal or ventral end) since that was previously established as a standard (Iovine and Johnson, 2000). Student's t -tests were performed in Excel to determine if experimental conditions were significantly different from control conditions.

Regenerate and segment length was measured using ImagePro software. Fin ray length was measured from the amputation plane (clearly visible in bright field) to the end of the fin. Segment length is measured as the distance between two joints where joints are identified (i.e. and clearly distinguished from breaks) following ZNS5 staining (Sims et al., 2009).

The mitotic cells were first detected by H3P staining as described above (i.e. Histone-3 is phosphorylated on Ser10 only during mitosis, Wei et al., 1999). H3P positive cells were counted from within the distal-most 250 µm of each ray (Hoptak-Solga et al., 2008).

qRT-PCR analysis

qRT-PCR analysis was performed as described (Sims et al., 2009). In brief, Trizol reagent was used to isolate mRNA from 5 dpa wild-type, *sof*^{b123}, or *alf*^{dy86} regenerating fins and 1 dpe (i.e. *cx43*-knockdown fins) (5 fins per pool). First strand cDNA was synthesized using oligodT (12–15) and reverse transcriptase. Dilution of template cDNA (1:10) was prepared. Oligos flanking introns were designed for *sema3d* (F-5' TGGATGAGGAGAGAAGCCGAT 3'; R-5' GCAGGCCAGCTCAACTTTT 3') using Primer Express software (primers for *cx43* and *keratin4* can be found in Sims et al., 2009). The *sema3d*, *cx43*, and *keratin4* amplicons were amplified independently using the Power SYBR green PCR master mix (Applied Biosystems). Samples were run in triplicate on the ABI7300 Real Time PCR system and the average cycle number (C_T) was determined for each amplicon. Delta C_T (ΔC_T) values represent normalized *sema3d* levels with respect to *keratin4*, the internal control. The relative level of gene expression was determined using the delta delta C_T ($\Delta\Delta C_T$) method (i.e. $2^{-\Delta\Delta C_T}$). A minimum of three trials were run to ensure the reproducibility of the results.

Results

Sema3d functions downstream of *cx43*

We completed a novel microarray strategy designed to identify genes acting downstream of *cx43*. We took advantage of our findings that *cx43* expression is reduced in *sof*^{b123} and increased in *alf*^{dy86} in order to identify a group of genes that are both down-regulated when *cx43* is down-regulated (i.e. in *sof*^{b123}) and up-regulated when *cx43* is up-regulated (i.e. in *alf*^{dy86}). Importantly, the *cx43* gene is found among the top 50 genes identified using this strategy, strongly suggesting that this approach identified relevant genes of interest (supplemental data, Table S1). Another gene found in the top half of the microarray was the secreted semaphorin gene, *sema3d*. Given the importance of semaphorins

in a diversity of signaling pathways, we were intrigued at the possibility that *Sema3d* signaling mediates Cx43 activities.

In order to validate *sema3d* as a downstream target of Cx43, we first examined *sema3d* expression in wild-type, *sof^{fb123}* and *alf^{dy86}* regenerating fins by whole mount in situ hybridization. As anticipated, *sema3d* mRNA expression appeared down-regulated in *sof^{fb123}* and up-regulated in *alf^{dy86}* (Fig. 1). Next, we determined the tissue-specific expression of *sema3d* as revealed by cryosectioning. The outer cell layers of the fin are epidermis; the basal layer of the epidermis is identified as a row of cuboidal-shaped cells closest to the mesenchymal compartment. Within the mesenchyme, the skeletal precursor cells (i.e. pre-osteoblasts and pre-joint-forming cells) are located laterally. The regeneration blastema, the specialized population of dividing cells contributing to new fin outgrowth, is medially adjacent to the skeletal precursors. This population of cells up-regulates *cx43* expression during fin regeneration (Hoptak-Solga et al., 2008). In contrast, cryosectioning of stained *sema3d*-positive fins revealed that *sema3d* is expressed in both the lateral skeletal precursor cells and in the lateral basal layer of the epidermis (Fig. 1). Since *sema3d* expression is not up-regulated in the *cx43*-positive cells, *sema3d* appears not to be a direct target of Cx43 activity.

To confirm the observed qualitative differences in *sema3d* expression we performed quantitative RT-PCR (qRT-PCR). We find that *sema3d* is reduced in *sof^{fb123}* and increased in *alf^{dy86}* (Table 2). Moreover, we find that *sema3d* expression is reduced in wild-type fins treated for *cx43*-knockdown, providing independent evidence

Table 2

Expression of *sema3d* via qRT-PCR.

Strain	Trial 1	Trial 2	Trial 3
Wild-type	1	1	1
<i>sof^{fb123}</i>	0.6	0.65	0.71
<i>alf^{dy86}</i>	1.95	1.42	1.90
<i>cx43</i> -KD fins	0.7	0.4	0.55

The fold-difference with respect to wild-type is shown for each of three trials.

that *sema3d* expression is influenced by Cx43 activity. Together, these data support the hypothesis that *sema3d* expression is regulated by the level of Cx43.

Sema3d mediates Cx43-dependent cell proliferation and joint formation

To determine if *sema3d* mediates Cx43-dependent phenotypes, we completed morpholino-mediated gene knockdown of *sema3d* (as described for *cx43* knockdown in Hoptak-Solga et al., 2008 and in Sims et al., 2009). Briefly, fins were injected with either a gene-specific targeting morpholino (MO) or with an altered morpholino that includes five mismatches (MM) to the target sequence. Following injection into the distal region of the regenerate, fins were electroporated to permit cellular uptake. Morpholinos were modified with fluorescein, which both provides a requisite charge for electroporation and provides a method to confirm cellular uptake. Interestingly, we find that *sema3d*-knockdown exhibits all of the same loss-of-function phenotypes as *sof^{fb123}* mutants (Iovine et al., 2005; Hoptak-Solga et al., 2008) and as *cx43*-knockdown (Hoptak-Solga et al., 2008; Sims et al., 2009). Thus, *sema3d* knockdown fins exhibit reduced fin length, reduced segment length, and reduced cell proliferation (Fig. 2A–C and Fig. 3 for representative images). The level of cell proliferation was evaluated by counting the number of cells in mitosis, and detected using an antibody against histone-3-phosphate (i.e. H3P). These data demonstrate that *sema3d* mediates *cx43*-dependent fin phenotypes influencing growth and joint formation. To provide additional evidence that *sema3d* functions in a common pathway with *cx43*, we next attempted to rescue the joint formation phenotype of *alf^{dy86}*. Indeed, *sema3d* knockdown rescued the joint failure phenotype of *alf^{dy86}*, causing reduced segment length (Fig. 2D). Until now, only reduced *cx43* function has been associated with segment length phenotypes and with rescue of joint formation in *alf^{dy86}*. Therefore, the finding that *sema3d* knockdown caused short segments in wild-type and rescued segment length in *alf^{dy86}* is striking. Together these data indicate that *cx43* and *sema3d* function in a common pathway to regulate cell proliferation and joint formation. Thus, *Sema3d* signaling mediates Cx43-specific effects.

Identification of putative *Sema3d* receptors

Neuropilins (Nrps) and Plexins (Plxns) are likely receptors for Semaphorin signaling (reviewed in Zhou et al., 2008). Indeed, Nrps and Plxns may hetero-oligomerize to transduce *Sema* signals. Nrps are believed to bind *Semas* directly (although Plxns also contain a *sema* domain), but have a very short intracellular domain that may not be sufficient to transduce intracellular signals. Plxns, on the other hand, have an extensive intracellular domain (reviewed in Zhou et al., 2008). Since both Nrps and Plxns are the best known receptors for *Semas*, we initiated a candidate gene search of these gene families. The zebrafish genome contains 4 *neuropilin* (*nrp*) genes (*nrp1a*, *nrp1b*, *nrp2a*, and *nrp2b*, Yu et al., 2004). In addition, Plexins in the A and D families are candidate receptors for secreted *Semas* (Zhou et al., 2008). The zebrafish genome contains *plexina1*

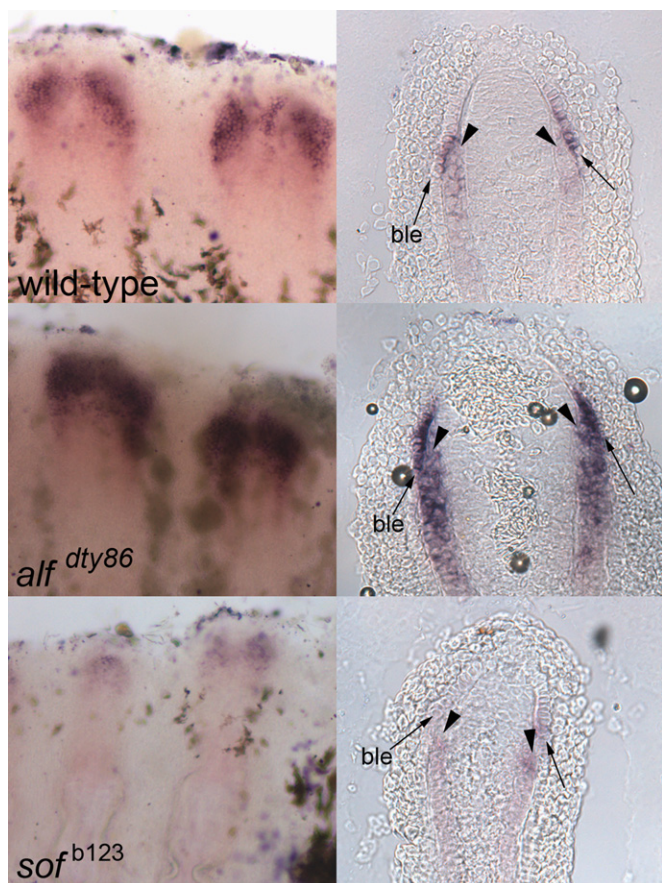


Fig. 1. *sema3d* is differentially expressed in wild-type (top), *alf^{dy86}* (middle) and *sof^{fb123}* (bottom). Left: whole mount in situ hybridization shows increased expression in *alf^{dy86}* and decreased expression in *sof^{fb123}* compared to wild-type. Right: Cryosections reveal the tissue-specific localization of *sema3d*-expressing cells. Arrowheads point to skeletal precursor cells; arrows point to the basal layer of the epidermis (ble).

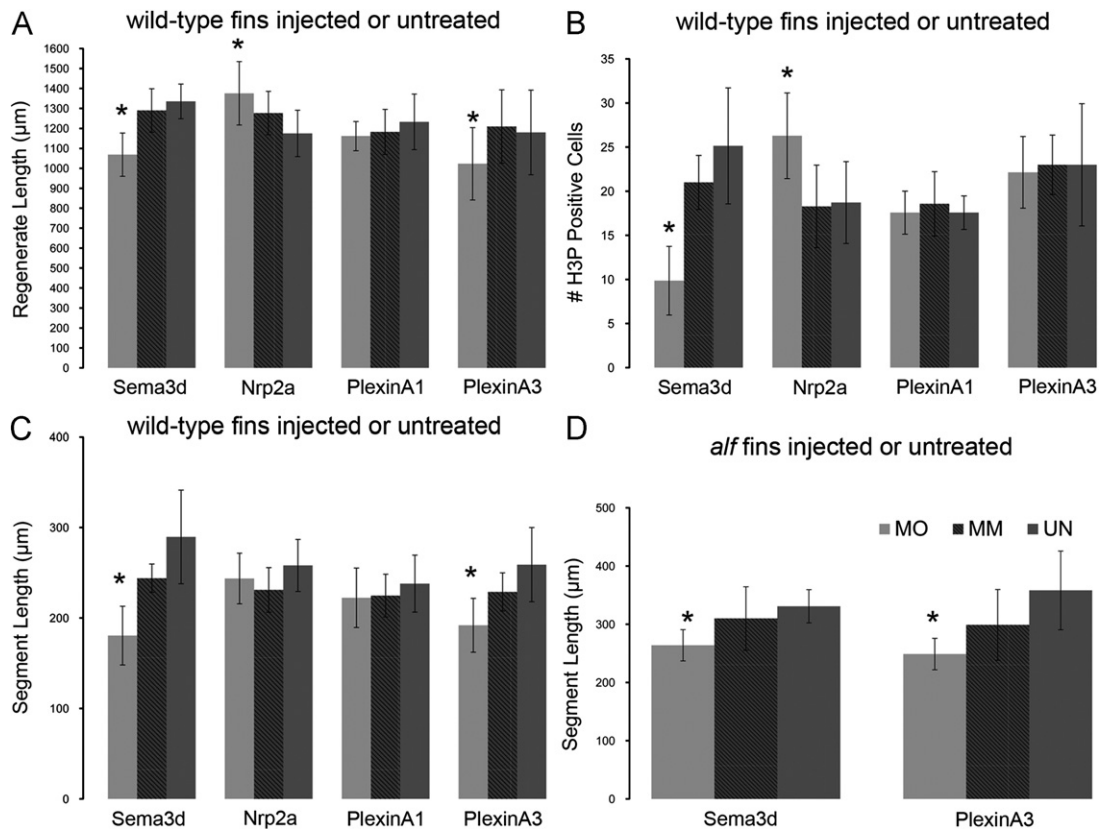


Fig. 2. Morpholino-mediated gene knockdown of *sema3d* and its putative receptors. In all graphs, MO represents the particular gene-targeting morpholino; MM represents the particular 5 mis-match/control morpholino; UN represents uninjected/untreated fins. (A) Total regenerate length was measured. *sema3d*-knockdown and *plxna3*-knockdown cause reduced fin length (*); *nrp2a*-knockdown causes increased fin length (*). (B) the total number of H3P positive cells were counted. *sema3d*-knockdown causes reduced levels of cell proliferation (*); *nrp2a*-knockdown causes increased levels of cell proliferation (*). (C) segment length was measured in treated wild-type fins. *sema3d*-knockdown and *plxna3*-knockdown cause reduced segment length (*) and (D) segment length was measured in treated *alf^{dy86}* fins. *sema3d*-knockdown and *plxna3*-knockdown cause reduced segment length and rescue joint formation in *alf^{dy86}* (*). Statistically different data sets (*) were determined by the student's *t*-test where $p < 0.05$. By the student's *t*-test, there is no statistical difference between MM and UN for any mismatch morpholino. Error bars represent the standard deviation.

(*plxna1*), *plxna3*, *plxna4*, and *plxnd1*. Of these 8 candidate genes, only *nrp2a*, *plxna1*, and *plxna3* appear to be expressed in regenerating fins by in situ hybridization (Fig. 4). The expression of *nrp2a* appears mainly in the blastema, perhaps more heavily localized distally. The distal-most blastema has been proposed to regulate fin outgrowth during regeneration (Nechiporuk and Keating, 2002). There is also apparent staining in the skeletal precursor cells, and sporadic but strong staining in individual cells of the outer layers of the epithelium. The identity of these cells is not known. The *plxna1* gene is expressed primarily in the distal blastema and also in the distal basal layer of the epidermis. In contrast, *plxna3* appears to be expressed primarily in the skeletal precursor cells and throughout the medial compartment of the regenerate.

PlxnA3 and Nrp2a mediate independent Sema3d functions

Next we completed functional analyses to determine which, if any, of these receptors contribute to the Cx43-Sema3d pathway. Receptors that mediate Sema3d function are expected to exhibit similar knockdown phenotypes as *cx43* and *sema3d*. However, knockdown of *plxna1* did not appear to influence either cell proliferation or joint formation (Figs. 2 and 3), suggesting that *PlxnA1* does not participate in Cx43-Sema3d-dependent skeletal morphogenesis. In contrast, knockdown of *plxna3* caused short segments (Fig. 2C and Fig. 3) but had no effect on cell proliferation (Fig. 2B). There is some influence of *plxna3* knockdown on fin length, as the length of the regenerate was statistically shorter than the controls

(Fig. 2A). Since there was no effect on cell proliferation, we conclude that the small *plxna3*-dependent effect on fin length is due to its influence on segment length, and not on fin growth. To provide further support for the functional relationship between *PlxnA3* and *cx43*-dependent joint formation, we evaluated the effect of *plxna3*-knockdown in *alf^{dy86}* regenerating fins. As anticipated, *plxna3*-knockdown rescued the joint formation phenotype, recapitulating the *cx43*- and *sema3d*-knockdown effects (Fig. 2D). These data suggest that *PlxnA3* contributes to Sema3d-mediated joint formation. Therefore, we have now identified a third gene (i.e. *plxna3*), predicted to function downstream of Cx43-Sema3d, whose function is required for appropriate joint formation.

Knockdown of *nrp2a* caused increased fin growth and increased cell proliferation (Fig. 2A and B and Fig. 3), suggesting that signaling via *Nrp2a* negatively influences cell division. There was no effect on segment length following *nrp2a* gene knockdown (Fig. 2C), indicating that *Nrp2a* signaling does not mediate Sema3d effects on joint formation. Since knockdown of *cx43* and *sema3d* both cause reduced growth and reduced cell proliferation, it was anticipated that *Nrp2a* knockdown would similarly cause reduced growth and cell proliferation. Since this was not the case, we suggest instead that Sema3d binding to the *Nrp2a* receptor inactivates its activity, thereby positively regulating cell division by inhibiting a negative signal. We attempted to provide evidence for this hypothesis by evaluating *Nrp2a* knockdown in *sof^{b123}* fins, which express less *sema3d* (Fig. 1 and Table 2). For example, if Sema3d is required to block the effects of *Nrp2a* signaling, then the increase in cell proliferation associated with *Nrp2a*

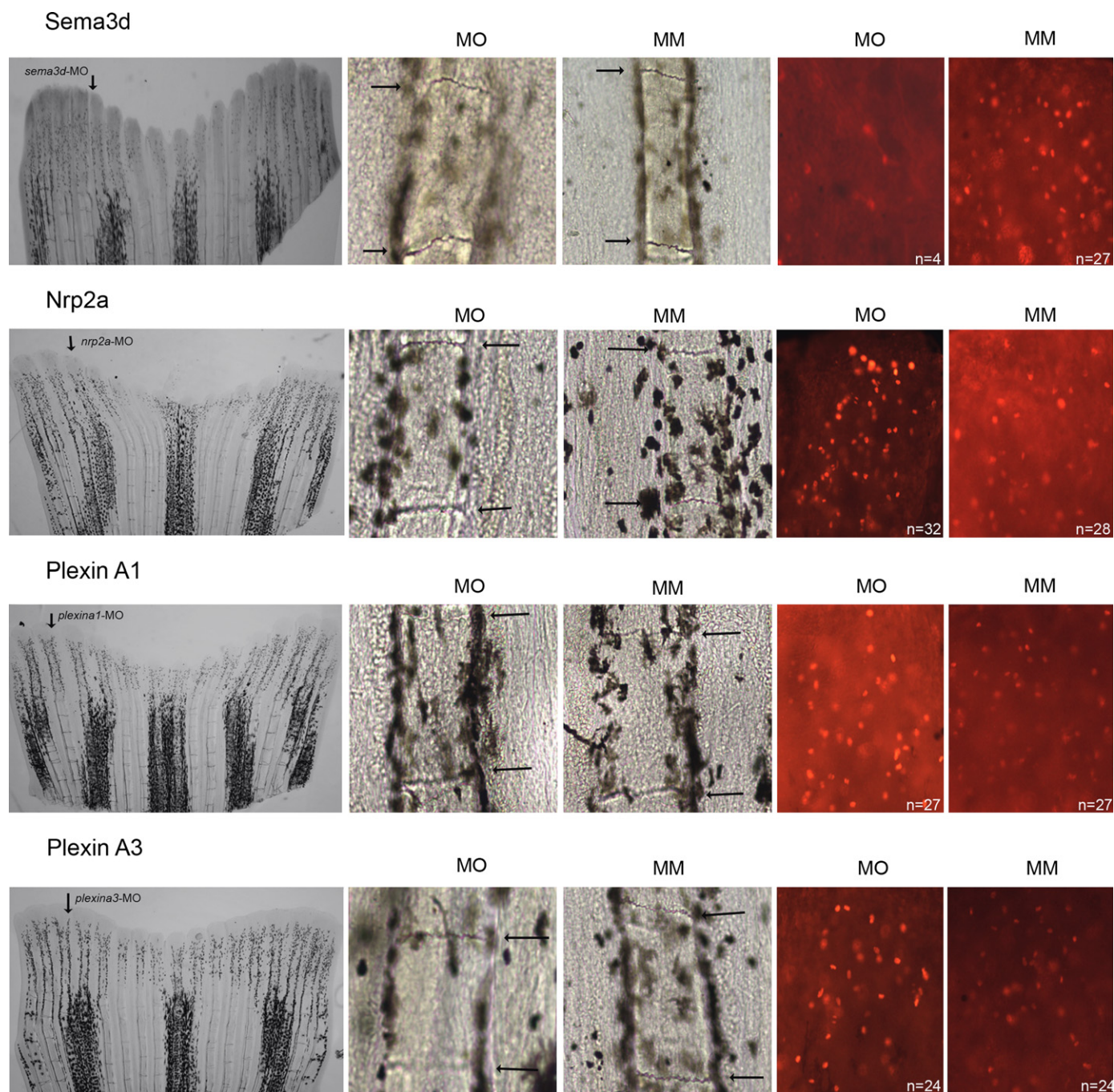


Fig. 3. Representative images of morpholino-induced phenotypes. From left to right: representative whole fins following injection in the dorsal-most 5–6 fin rays (arrow); segment length in targeting morpholino-injected (MO) and in 5 mis-match morpholino-injected (MM); H3P-positive cells in targeting morpholino-injected (MO) and in 5 mis-match morpholino-injected (MM).

knockdown should be attenuated when *Sema3d* is reduced, as in *sof^{b123}*. This is what we find. *Nrp2a* knockdown in wild-type regenerating fins causes a 30% increase in dividing cells, while *Nrp2a* knockdown in *sof^{b123}* regenerating fins has no effect on the number of dividing cells (Fig. 5). Further studies will be required to demonstrate unequivocally that *Sema3d* acts as a ligand for *Nrp2a*. However, our current findings provide support for the conclusion that *Sema3d* can mediate negative regulation of *Nrp2a* and thereby promote cell proliferation. Note that the observed *Nrp2a* effects may be mediated in conjunction with an as yet

unidentified Plxn co-receptor since Nrps appear not to encode intracellular signaling domains.

Together, our analyses of the *plxna1*, *plxna3*, and *nrp2a* genes suggest that *Nrp2a* and *PlxnA3* mediate *Sema3d*-dependent events, while *PlxnA1* does not appear to function in *Sema3d*-mediated events. Moreover, we suggest that *Nrp2a* and *PlxnA3* mediate distinct Cx43- and *Sema3d*-dependent phenotypes, where *Nrp2a* mediates the Cx43-dependent effects on cell proliferation and *PlxnA3* mediates the Cx43-dependent effects on joint formation.

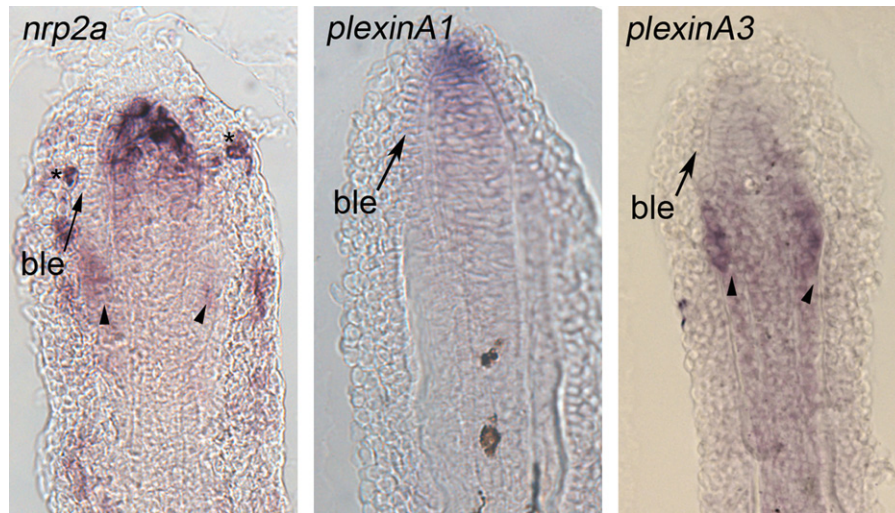


Fig. 4. Gene expression of candidate receptors for Sema3d. Left: expression of *nrp2a* is primarily located in the distal blastema and in skeletal precursor cells. Staining of individual cells of the outer epithelial cells is also observed (*). Middle: expression of *plxna1* is primarily in the distal blastema and in the distal cells of the basal epidermis. Right: expression of *plxna3* is located in both the skeletal precursor cells and in the blastema. Arrows identify the basal layer of the epidermis (ble), arrowheads identify skeletal precursor cells.

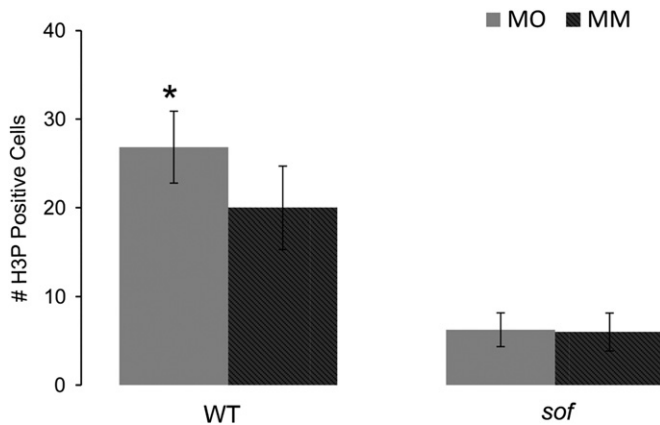


Fig. 5. Nrp2a-knockdown effects are abrogated in *sof*^{h123}. Nrp2a-mediated gene knockdown causes an increase in cell proliferation when Sema3d is present at typical levels. In *sof*^{h123}, where *sema3d* expression is reduced, Nrp2a is unable to enhance the level of cell proliferation. MO, gene-targeting morpholino. MM, 5 mismatch/control morpholino.

Discussion

Much of what is known about *sema3d* has been determined during development of the central nervous system in zebrafish. In the embryonic nervous system *sema3d* has been found to exert multiple diverse functions. For example, *sema3d* may act as an axonal repellent or as an axonal attractant (Wolman et al., 2004). Alternatively, *sema3d* function can modify cell adhesion via influencing the expression of the adhesion protein L1 (Wolman et al., 2007). Further, *sema3d* has been found to influence the population of neural crest cells by promoting proliferation (Berndt and Halloran, 2006), and by regulating their migration (Yu and Moens, 2005). It has been suggested that the different functions of *sema3d* may depend on the receptors expressed on the responding cells. Indeed, depending on the cell-type, *sema3d* has been found to interact with *nrp1a* (Wolman et al., 2004), with *nrp1a/nrp2b* (Wolman et al., 2004), or via *nrp*-independent mechanisms (Wolman et al., 2007). Thus, Sema3d appears to interact with a variety of receptors in order to mediate a diversity of downstream cellular events. It is therefore not possible to predict a specific receptor complement/pathway for Sema3d

function. However, it is also not difficult to envision how Sema3d signaling could be responsible for mediating multiple independent signaling events during fin regeneration.

The finding that Sema3d functions downstream of Cx43 is supported by multiple independent lines of evidence. First, the *sema3d* gene exhibits differential expression in *sof*^{h123} and *alf*^{dy86} regenerating fins by in situ hybridization and by qRT-PCR. Second, *cx43*-knockdown in wild-type fins is sufficient to reduce *sema3d* gene expression. Third, we provide functional evidence that *sema3d* acts downstream of *cx43* since *sema3d*-knockdown recapitulates all of the *cx43*-dependent phenotypes, including rescue of joint formation in *alf*^{dy86}. Thus, *sema3d* is both molecularly and functionally downstream of Cx43. Moreover, we identify two putative Sema3d receptors, Nrp2a and PlxnA3. Remarkably, these receptors appear to independently mediate Cx43-Sema3d-dependent cell proliferation and joint formation. The described functional analyses for Sema3d and its putative receptors utilized translation-blocking morpholinos. Since antibodies are not currently available, we are unable to demonstrate that protein translation of the targets is inhibited following morpholino-mediated gene knockdown. However, the specificity of *sema3d*- and *plxna3*- knockdown to Cx43-dependent phenotypes is provided by our findings that *sema3d*- and *plxna3*-knockdown both cause short segments and also rescue joint failure in *alf*^{dy86} (i.e. prior to this report, these findings were specific for *cx43* mutations or knockdown). Similarly, the finding that *sof*^{h123} abrogates the effects of *nrp2a*-knockdown provides specificity for the role of Nrp2a in Cx43-Sema3d-dependent cell proliferation. We did not observe Cx43-dependent phenotypes following *plxna1*-knockdown. However, until we can demonstrate that the PlxnA1 protein has been successfully reduced, we cannot formally rule out the possibility that PlxnA1 also contributes to Sema3d signaling events.

Based on our current and published findings (summarized in Table 3), we suggest the following model for Cx43 activity during fin regeneration (Fig. 6). Prior studies from our lab have shown that Cx43 both promotes cell proliferation and suppresses joint formation (Hoptak-Solga et al., 2008; Sims et al., 2009). Here we find that Sema3d signaling contributes to these Cx43-dependent activities in a pathway that bifurcates after Sema3d (Fig. 6A). Indeed, functional analyses of Cx43 and Sema3d provide evidence that cell proliferation and joint formation are coupled, while functional analyses of the putative Sema3d receptors

Table 3
Phenotypes associated with altered expression of Cx43 and genes proposed to function downstream of Cx43.

Mutant/ morphant	<i>cx43</i>	<i>sema3d</i>	Fin length	Segment length	Cell proliferation
<i>sof^{h123}</i>	low	low	short	short	reduced
<i>alf^{dy86}</i>	high	high	long	long	increased
<i>cx43-KD</i>	low	low	short	short	reduced
<i>sema3d-KD</i>	n/c	low	short	short	reduced
<i>plxna3-KD</i>	n/d	n/d	short	short	n/c
<i>nrp2a-KD</i>	n/d	n/d	long	n/c	increased

Changes in *cx43* and *sema3d* gene expression were evaluated by qRT-PCR. All knockdowns (KD) listed were completed in wild-type regenerating fins. No change (n/c); not done (n/d).

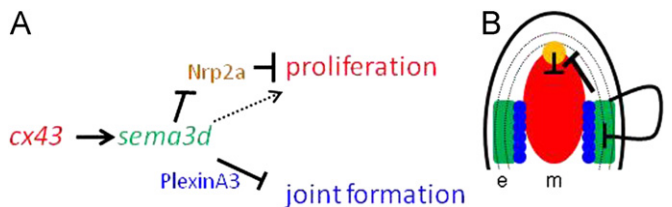


Fig. 6. Model of how Cx43-Sema3d influences skeletal morphology. (A) Proposed pathway of Cx43-Sema3d and downstream receptors (text colors are coordinated with the cartoon in B). Cx43 activity in the dividing cells influences *sema3d* gene expression in the lateral skeletal precursors and basal layer of the epidermis. Secreted Sema3d promotes cell proliferation (dotted arrow) in the *cx43*-positive compartment by inhibiting a negative signal from Nrp2a in the distal blastema. Sema3d suppresses joint formation in the skeletal precursor cells by its interaction with PlxnA3. (B) cartoon illustrating the compartments of gene expression in the Cx43-Sema3d pathway (e, epithelium; m, mesenchyme; basal layer of the epidermis is dotted). The *cx43* mRNA is up-regulated in the blastema (red), adjacent to the *sema3d*-positive cells in the skeletal precursor cells and in the lateral basal layer of the epidermis (green). Cx43-dependent up-regulation of *sema3d* in the lateral compartment allows secreted Sema3d to signal back to the blastema via Nrp2a (yellow), relieving the Nrp2a inhibition of cell proliferation. Sema3d signaling via PlxnA3 in the skeletal precursor cells (blue circles) inhibits joint formation in the skeletal precursor cells, perhaps by influencing osteoblast/joint-forming cell differentiation.

demonstrate effects on either cell proliferation (i.e. Nrp2a) or joint formation (i.e. PlxnA3). Thus, Cx43 coordinates skeletal growth and patterning via Sema3d signaling, which in turn regulates cell proliferation and joint formation in distinct downstream signaling pathways.

It is possible to visualize the steps of this molecular pathway by considering the location of gene expression of the molecular players (Fig. 6B). For example, Cx43 is expressed in the medially located dividing cells during fin regeneration (Iovine et al., 2005). These cells are directly adjacent to the skeletal precursor cells that will differentiate as either osteoblasts or joint forming cells (Brown et al., 2009; Borday et al., 2001). We suggest that Cx43 activity in the dividing cells influences gene expression of *sema3d* in the adjacent lateral compartments, which in turn mediates independent signaling pathways that regulate cell division and joint formation. It remains unknown how gap junctions contribute to tangible changes in gene expression. One possibility is that Cx43-dependent GJIC influences the concentration of a second messenger that directly regulates the activity of a relevant transcription factor in the *cx43*-positive cells. These changes in gene expression in the *cx43*-positive compartment lead to changes in gene expression in the adjacent *sema3d*-positive compartment. Once the expression of *sema3d* is up-regulated in the lateral skeletal precursor cells, Sema3d will be secreted where it may interact with its receptors. Conveniently, Nrp2a and PlxnA3, which mediate independent events, are expressed in

distinct populations of cells. For example, the Nrp2a receptor is expressed in the distal blastema where it may influence cell proliferation in the *cx43*-positive cells. We suggest that Sema3d binding to Nrp2a prevents the inhibition of cell proliferation, thereby promoting growth. Similarly, the expression of *plxna3* in the skeletal precursor cells suggests that secreted Sema3d binds to the PlxnA3 receptor and initiates an autocrine response to influence the expression of genes that will determine joint formation (i.e. promoting osteoblast differentiation, suppressing joint formation, or both). However, recall that *nrp2a* and *plxna3* are expressed in more than one cellular compartment during fin regeneration. Thus, it remains possible that Sema3d signaling events are more complicated than this model suggests.

The model we propose suggests that Sema3d initiates a typical signal transduction pathway that directly influences cell proliferation or joint formation in the cells expressing the putative receptors. This model is consistent with our examination of gene expression patterns and on functional analyses. Alternate models are also possible. For example, it has been suggested that Sema3A influences innervation and/or vascularization of endochondral bones in mammals, which in turn impacts bone growth (Gomez et al., 2005). The fin rays contain both nerve axons and blood vessels, although it is not known if Sema3d and/or its receptors are expressed in either of those cell populations. Future immunohistochemical analyses may provide new insights into the possibility that Cx43-Sema3d drives growth and/or patterning via the vasculature or nervous system. Moreover, others have found evidence that Sema3F may influence the localization of Cx43 to the plasma membrane in rat liver epithelial cell lines, perhaps regulating Cx43-based GJIC (Kawasaki et al., 2007). Our findings do not support this type of role for Sema3d during fin regeneration since *cx43* and *sema3d* are not co-expressed in the same population of cells. However, it remains possible that additional Semas may contribute to the expression and/or localization of Cx43.

Conclusions

The identification of Sema3d acting downstream of Cx43 provides tangible insights into how cellular outcomes are coupled in order to coordinate bone growth with skeletal patterning. We find that the Cx43-Sema3d pathway diverges via distinct receptors to influence two cellular outcomes: cell proliferation and joint formation. Continued validation of additional genes identified by our microarray will fill the gaps of molecular events occurring both between Cx43 activity and Sema3d signaling as well as events occurring downstream of the putative Sema3d receptors that mediate changes in cell division and joint formation.

Acknowledgments

The authors would like to thank Rebecca Jefferis for maintenance and care of the fish colony, and members of the Iovine lab for critical discussions regarding this manuscript. Isha Jain completed the microarray analysis in collaboration with Dr. Jutta Marzillier. This research was funded in part from the NIH (HD047737) and by Lehigh's Department of Biological Sciences. The ZNS5 antibody was purchased from the Zebrafish International Resource Center, which is supported by P40 RR12546.

Appendix A. Supporting information

Supplementary data associated with this article can be found in the online version at <http://dx.doi.org/10.1016/j.ydbio.2012.03.020>.

References

- Berndt, J.D., Halloran, M.C., 2006. Semaphorin 3d promotes cell proliferation and neural crest cell development downstream of TCF in the zebrafish hindbrain. *Development* 133, 3983–3992.
- Borday, V., Thaeron, C., Avaron, F., Brulfert, A., Casane, D., Laurenti, P., Geraudie, J., 2001. *evx1* transcription in bony fin rays segment boundaries leads to a reiterated pattern during zebrafish fin development and regeneration. *Dev. Dyn.* 220, 91–98.
- Brown, A.M., Fisher, S., Iovine, M.K., 2009. Osteoblast maturation occurs in overlapping proximal-distal compartments during fin regeneration in zebrafish. *Dev. Dyn.* 238, 2922–2928.
- Flenniken, A.M., Osborne, L.R., Anderson, N., Ciliberti, N., Fleming, C., Gittens, J.E., Gong, X.Q., Kelsey, L.B., Lounsbury, C., Moreno, L., Nieman, B.J., Peterson, K., Qu, D., Roscoe, W., Shao, Q., Tong, D., Veitch, G.L., Voronina, I., Vukobradovic, I., Wood, G.A., Zhu, Y., Zirngibl, R.A., Aubin, J.E., Bai, D., Bruneau, B.G., Grynopas, M., Henderson, J.E., Henkelman, R.M., McKelvie, C., Sled, J.G., Stanford, W.L., Laird, D.W., Kidder, G.M., Adamson, S.L., Rossant, J., 2005. A *Gja1* missense mutation in a mouse model of oculodentodigital dysplasia. *Development* 132, 4375–4386.
- Gomez, C., Burt-Pichat, B., Mallein-Gerin, F., Merle, B., Delmas, P.D., Skerry, T.M., Vico, L., Malaval, L., Chenu, C., 2005. Expression of Semaphorin-3A and its receptors in endochondral ossification: potential role in skeletal development and innervation. *Dev. Dyn.* 234, 393–403.
- Hoptak-Solga, A.D., Klein, K.A., Derosa, A.M., White, T.W., Iovine, M.K., 2007. Zebrafish short fin mutations in connexin43 lead to aberrant gap junctional intercellular communication. *FEBS Lett.* 581, 3297–3302.
- Hoptak-Solga, A.D., Nielsen, S., Jain, I., Thummel, R., Hyde, D.R., Iovine, M.K., 2008. Connexin43 (GJA1) is required in the population of dividing cells during fin regeneration. *Dev. Biol.* 317, 541–548.
- Iovine, M.K., Higgins, E.P., Hindes, A., Coblitz, B., Johnson, S.L., 2005. Mutations in connexin43 (GJA1) perturb bone growth in zebrafish fins. *Dev. Biol.* 278, 208–219.
- Iovine, M.K., Johnson, S.L., 2000. Genetic analysis of isometric growth control mechanisms in the zebrafish caudal fin. *Genetics* 155, 1321–1329.
- Kawasaki, Y., Kubomoto, A., Yamasaki, H., 2007. Control of intracellular localization and function of Cx43 by SEMA3F. *J. Membr. Biol.* 217, 53–61.
- Kolodkin, A.L., Matthes, D.J., O'Connor, T.P., Patel, N.H., Admon, A., Bentley, D., Goodman, C.S., 1992. Fasciclin IV: sequence, expression, and function during growth cone guidance in the grasshopper embryo. *Neuron* 9, 831–845.
- Lecanda, F., Warlow, P.M., Sheikh, S., Furlan, F., Steinberg, T.H., Civitelli, R., 2000. Connexin43 deficiency causes delayed ossification, craniofacial abnormalities, and osteoblast dysfunction. *J. Cell Biol.* 151, 931–944.
- Lee, Y., Grill, S., Sanchez, A., Murphy-Ryan, M., Poss, K.D., 2005. Fgf signaling instructs position-dependent growth rate during zebrafish fin regeneration. *Development* 132, 5173–5183.
- Nechiporuk, A., Keating, M.T., 2002. A proliferation gradient between proximal and msxb-expressing distal blastema directs zebrafish fin regeneration. *Development* 129, 2607–2617.
- Paznekas, W.A., Boyadjiev, S.A., Shapiro, R.E., Daniels, O., Wollnik, B., Keegan, C.E., Innis, J.W., Dinulos, M.B., Christian, C., Hannibal, M.C., Jabs, E.W., 2003. Connexin 43 (GJA1) mutations cause the pleiotropic phenotype of oculodentodigital dysplasia. *Am. J. Hum. Genet.* 72, 408–418.
- Quint, E., Smith, A., Avaron, F., Laforest, L., Miles, J., Gaffield, W., Akimenko, M.A., 2002. Bone patterning is altered in the regenerating zebrafish caudal fin after ectopic expression of sonic hedgehog and *bmp2b* or exposure to cyclopamine. *Proc. Natl. Acad. Sci. U S A* 99, 8713–8718.
- Roth, L., Koncina, E., Satkauskas, S., Cremel, G., Aunis, D., Bagnard, D., 2009. The many faces of semaphorins: from development to pathology. *Cell Mol. Life Sci.* 66, 649–666.
- Sims Jr., K., Eble, D.M., Iovine, M.K., 2009. Connexin43 regulates joint location in zebrafish fins. *Dev. Biol.* 327, 410–418.
- Stains, J.P., Lecanda, F., Screen, J., Towler, D.A., Civitelli, R., 2003. Gap junctional communication modulates gene transcription by altering the recruitment of Sp1 and Sp3 to connexin-response elements in osteoblast promoters. *J. Biol. Chem.* 278, 24377–24387.
- Thummel, R., Bai, S., Sarrajs Jr., M.P., Song, P., McDermott, J., Brewer, J., Perry, M., Zhang, X., Hyde, D.R., Godwin, A.R., 2006. Inhibition of zebrafish fin regeneration using in vivo electroporation of morpholinos against *fgfr1* and *msxb*. *Dev. Dyn.* 235, 336–346.
- van Eeden, F.J., Granato, M., Schach, U., Brand, M., Furutani-Seiki, M., Haffter, P., Hammerschmidt, M., Heisenberg, C.P., Jiang, Y.J., Kane, D.A., Kelsh, R.N., Mullins, M.C., Odenthal, J., Warga, R.M., Nusslein-Volhard, C., 1996. Genetic analysis of fin formation in the zebrafish, *Danio rerio*. *Development* 123, 255–262.
- Wei, Y., Yu, L., Bowen, J., Gorovsky, M.A., Allis, C.D., 1999. Phosphorylation of histone H3 is required for proper chromosome condensation and segregation. *Cell* 97, 99–109.
- Westerfield, M., 1993. *The Zebrafish Book: A guide for the laboratory use of zebrafish (Brachydanio rerio)*. University of Oregon Press, Eugene, OR.
- Wolman, M.A., Liu, Y., Tawarayama, H., Shoji, W., Halloran, M.C., 2004. Repulsion and attraction of axons by semaphorin3D are mediated by different neuropilins in vivo. *J. Neurosci.* 24, 8428–8435.
- Wolman, M.A., Regnery, A.M., Becker, T., Becker, C.G., Halloran, M.C., 2007. Semaphorin3D regulates axon axon interactions by modulating levels of L1 cell adhesion molecule. *J. Neurosci.* 27, 9653–9663.
- Yazdani, U., Terman, J.R., 2006. The semaphorins. *Genome Biol.* 7, 211.
- Yu, H.H., Houart, C., Moens, C.B., 2004. Cloning and embryonic expression of zebrafish neuropilin genes. *Gene Expression Patterns* 4, 371–378.
- Yu, H.H., Moens, C.B., 2005. Semaphorin signaling guides cranial neural crest cell migration in zebrafish. *Dev. Biol.* 280, 373–385.
- Zhou, Y., Gunput, R.A., Pasterkamp, R.J., 2008. Semaphorin signaling: progress made and promises ahead. *Trends Biochem. Sci.* 33, 161–170.